JACS
JOURNAL OF THE AMERICAN CHEMICAL SOCIETY

Article

pubs.acs.org/JACS

Bimodal Gold Nanoparticle Therapeutics for Manipulating Exogenous and Endogenous Protein Levels in Mammalian Cells

Megan E. Muroski, Joshua M. Kogot,[†] and Geoffrey F. Strouse*

Department of Chemistry and Biochemistry and Institute for Molecular Biophysics, The Florida State University, Florida 32306-4390, United States

Supporting Information

ABSTRACT: A new advance in cell transfection protocol using a bimodal nanoparticle agent to selectively manipulate protein expression levels within mammalian cells is demonstrated. The nanoparticle based transfection approach functions by controlled release of gene regulatory elements from a 6 nm AuNP (gold nanoparticle) surface. The endosomal release of the regulatory elements from the nanoparticle surface results in endogenous protein knockdown simultaneously with exogenous protein expression for the first 48 h. The use of fluorescent proteins as the endogenous and exogenous signals for protein expression enables the efficiency of codelivery of siRNA (small interfering RNA) for GFP (green fluorescent protein) knockdown and a dsRed-express linearized plasmid for induction to be optically analyzed in CRL-2794, a human kidney cell line expressing an unstable green fluorescent protein. Delivery of the bimodal nanoparticle in cationic liposomes results in 20% GFP knockdown within 24 h of delivery and continues exhibiting knockdown for up to 48 h for the bimodal agent. Simultaneous dsRed expression is observed to initiate within the same time frame with expression levels reaching 34% after 25 days although cells have divided approximately 20 times, implying daughter cell transfection has occurred. Fluorescence cell sorting results in a stable colony, as demonstrated by Western blot analysis. The simultaneous delivery of siRNA and linearized plasmid DNA on the surface of a single nanocrystal provides a unique method for definitive genetic control within a single cell and leads to a very efficient cell transfection protocol.

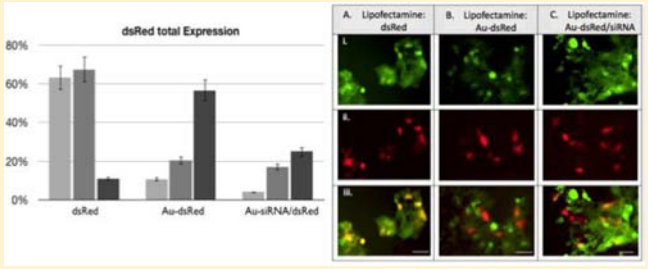

INTRODUCTION

The efficient delivery and function of genetic regulatory components, i.e., gene, siRNA (small interfering RNA), or mRNA, following cell transfection represents one of the many important steps for regulating exogenous and endogenous protein expression in mammalian cells.[1−8] Standard transfection approaches are often tedious or require optimization due to the high propensity for endosomal damage of the regulatory component once transfected into a cell. Although nucleic acid based therapeutic methods hold great promise, they is plagued by pharmacokinetic difficulties arising from the lack of efficient delivery, low level of endosomal escape, susceptibility to degradation, and cytotoxicty.[9]

Regulating exogenous and endogenous protein expression so they function on a similar time scale can open new therapeutic strategies if the function of siRNA can be delayed so that the gene induction of exogenous proteins can be timed to the down regulation of endogenous protein levels. To accomplish a coupled gene regulatory event, codelivery of the agents is needed. Codelivery of two agents (i.e., siRNA and a gene) in a liposome or independent delivery of separate transfection agents will result in stochastic response in the cells due to the vastly different loading levels for siRNA and a gene into transfection media. The stochastic response results in poor control over a desired metabolic outcome. Copackaging of the agents onto a single carrier allows the direct delivery of two or more agents into the same cell and can induce the concomitant down regulation of a protein and induced gene expression if the timing of these very different processes can be synchronized. Controlling the timing and magnitude of the response of delivered gene regulatory elements is difficult by standard transfection approaches since endosomal release and the processing of the agents, which occur on different time scales, impact the final metabolic outcome in the cell. Furthermore, delivering more than a single agent at a time is difficult due to the differences in the ability to package the agents, differences in the dynamics of endosomal escape following transfection, and differences in endosomal stability for a full gene vs siRNA.

Breakthroughs in codelivery may find applications in biomedical therapies in a wide range of disease. Simultaneously down-regulating a targeted protein while inducing an exogenous protein to express can have a significant impact in diseases. Such an approach to gene therapies could be utilized to impact disease states where a single point mutation in a protein causes deleterious effects; for instance, this strategy could be used to target disease such as AIDS and certain types of cancer.[5,9,10] Individuals afflicted with genetic disorders

Received: August 3, 2012
Published: November 6, 2012

   dx.doi.org/10.1021/ja307502x | J. Am. Chem. Soc. 2012, 134, 19722−19730

traceable to protein mutations (i.e., cystic fibrosis, sickle cell anemia) have the potential for improved well-being and longevity if the aberrant protein can be deliberately masked by controlled knockdown, while the wild-type form of the protein is transiently expressed.[11,12] If a generalized technique can be developed that is applicable to a single cell, a group of cells, or a whole organism, the results would lead to unprecedented opportunities to manipulate targeted protein levels within biomedically relevant cell lines or animal models.

Introducing gene regulatory elements based on siRNA, mRNA, and full genes into a mammalian cell exist in the literature.[13−18] Uptake of regulatory elements can be accomplished using viral, nonviral, or electroporation methods. Liposomes and chitosan exhibit low transfection efficiencies, while electroporation while viable for transfection often is accompanied by substantial cell death. Gene regulators based on viral vectors have been extensively reported, but the approach is frequently associated with immunogenic responses due to viral protein coat.[6,19−21] Nonviral delivery agents circumvent the endosomal barrier and include the use of liposomes, fusogenic lipids, polymers (proton sponge), encapsulation in a viral capsid,[17−20] packaging of siRNA in biodegradable polymers,[21−32] and electrostatic assemblies of siRNA with cell penetrating peptides. The use of nanoparticles to deliver either RNA or a full gene[22,23] into a cell to directly manipulate protein expression has garnered interest by the biomedical community.[2,8,24−28] When packaged at the surface of a nanoparticle, experiments by Mirkin et al. and others have shown that packaging of the siRNA onto a nanoparticle surface offers reduced nuclease activity, presumably due to a lack of accessibility.[3,29−31]

Utilizing a nanoparticle platform offers the potential to engineer a system capable of controlling the dosage level and duration of function for multiple gene therapeutics by codelivery of a gene for recombinant protein expression and a siRNA for knockdown.[8,32−38] By coassembling the gene and siRNA onto the same nanoparticle, the timing of activation is dependent upon the gene to release first due to packaging of the siRNA by the larger gene element. Although both down-regulation and induced protein expression have been demonstrated, no attempts to our knowledge have appeared that simultaneously down regulate an endogenous protein while inducing an exogenous protein expression, since it would be anticipated that the vastly different time scales for siRNA to knockdown protein expression and a delivered gene to induce protein expression would negate any advantage of codelivery. The coassembly of the siRNA and gene onto the AuNP (gold nanoparticle) surface results in delayed release of the siRNA from the NP surface presumably due to steric effects leading to the functioning of the agents on the same time scale

In this paper, we demonstrate the effectiveness of a bimodal agent designed to control endogenous and exogenous protein expression levels within CRL-2794, a human embryonic kidney cell line. Simultaneous gene regulation is demonstrated by coassembling onto a single 6 nm AuNP gene regulatory elements including siRNA (19 bp) designed to knockdown the native expression of GFP (green fluorescent protein) in CRL-2794 and a full length gene (4.7 kbp) intended to induce expression of dsRed within the cell. With the use of a set of distinct fluorescent protein signatures (green for endogenous, red for exogenous), the effectiveness of the bimodal agent to regulate protein expression within the CRL-2794 cell line can be optically imaged and statistically analyzed. Direct conjugation of the nucleic acid gene regulators to the AuNP surface is accomplished through an engineered 5′ C_6 thiol synthetic linker, which provides control over the amount of the regulatory elements within the cell and the prevention of dissociation and degradation of the agents prior to intracellular delivery.[24,39] The packaging of the gene and siRNA onto a single AuNP results in simultaneous gene regulation with down regulation of the native GFP by 20% for the bimodal agent for 48 h and 65% for the Au-siRNA agent at >24 h, while dsRed expression is initiated over the same time frame with 34% of the cells expressing dsRed 25 days after transfection. Cell sorting produces a stable colony for dsRed expression in the CRL-2794 cell line, as verified by Western blot analysis within weeks of transfection. By comparison, treatment with the gene or siRNA without the AuNP leads to high-level but short-term dsRed expression (67%, <72 h) and GFP knockdown (24 h, 30%).

The reported results represent a new approach to delivering regulatory elements simultaneously into a cell where the coassembly of the gene onto a nanoparticle surface in the presence of a covalently attached siRNA sequence results in delayed release of the siRNA, and, subsequently, the simultaneous activation of down-regulation and induction of protein expression within a cell. Developing new transfection strategies that utilize the nanoparticle to control delivery of genetic regulatory elements into a cell may at the minimum allow rapid establishment of biomedically relevant cell models, and potentially one day shift the approach for developing cell therapies.

EXPERIMENTAL SECTION

Chemicals. All chemicals utilized in the study were purchased from VWR. The siRNA and synthetic DNBA linker was purchased from Midland Corporation. The bacterial plasmid and Lipofectamine2000 is available from Invitrogen.

Synthesis of 6.0 nm, Spherical BSPP Passivated Gold Nanoparticle (AuNP). Buffer-soluble (PBS, pH = 7.2) 6 ± 0.8 nm AuNPs passivated by BSPP (bis(p-sulfonatophenyl)-phenylphosphine) are prepared by reduction of hydrogen tetrachloroaurate ($HAuCl_4{\cdot}3H_2O$) via the Frens method.[40] Briefly, a solution containing sodium citrate (1.4 mM) to tannic acid (0.03 mM) is added rapidly to a 0.25 mM $HAuCl_4$ solution in sparged H_2O at 60 °C. The mixture is allowed to stir for 5 min and cooled to RT, and an excess of BSPP is added to the solution to exchange the weakly coordinated citrate passivant. The AuNP is isolated by addition of saturated sodium chloride and centrifugation, washed with ethanol, and dried. The purity of the AuNP is analyzed by 1% agarose gel separation where a single band is observed to move in the gel (Supplemental Figure SF1A).

AuNP Characterization. AuNP size, dispersity, and morphology were analyzed on holey carbon (400 mesh) for NPs dispersed from a toluene solution by transmission electron microscopy (TEM) using a JEOL-2010 microscope operated at 200 kV. The isolated AuNP is spherical with a 13% size distribution analyzed for over 100 AuNPs (Supplemental Figure SF1B). The AuNP extinction spectra were measured by UV−vis spectroscopy in TBS buffer (pH 7.4) at ∼10^{-6} M concentrations in a 1-cm quartz cuvette using a Varian Cary 50 UV−vis spectrophotometer. The optical spectra indicate a well formed surface plasmon is visible for the gold at 525 nm (Supplemental Figure SF1C), consistent with Mie scattering theory predictions.[41]

5′ C_6-Thiol Functionalized dsRed-C1 Linearized Gene (4757 bp). The synthetically modified 5′ C_6-thiol functionalized dsRed-C1 linearized gene (S-dsRed) for appendage to the surface of the 6 nm gold nanoparticle is achieved by linearizing a commercially available dsRed-C1 plasmid (Clontech) by digestion with AflIII (New England Biolabs (NEB)) following the manufacturer's protocol. The dsRed-C1 gene contains a CMV (cytomegalovirus) promoter for protein overexpression, a dsRed fluorescent protein coding sequence for

dx.doi.org/10.1021/ja307502x | J. Am. Chem. Soc. 2012, 134, 19722−19730

visualization of transformation, and following linearization a *four* base pair overhang (CATG) to allow the ligation of the 5′ C_6-thiol functionalized synthetic DNA sequence required for attaching to the AuNP surface.

Ligation of the linearized gene fragment with the synthetic ds-DNA linker sequence containing a four base pair overhang and a 5′ phosphate C_6-disulfide modification (5′- CAT GCG ACT GTG ACA ATC TTA GCT GCC GAT AGA GTA GTC −3′ (39mer) 3′- GC TGA CAC TGT TAG AAT CGA CGG CTA TCT CAT CAG-SSH-5′ (35mer)) is carried out by T4 ligation of the 3′ cohesive end of the linker to the 5′ cohesive end of the linearized gene using standard protocols (New England Biolabs). The ligation is carried out in a 3 to 1 molar ratio of the synthetic linker to gene in T4 DNA ligase reaction buffer at 4 °C for 24 h, followed by deactivation of the T4 ligase by heating to 60 °C for 20 min, precipitation by addition of ethanol, centrifugation, and storage at −20 °C.

Preparation of the AuNP Gene Complex (Au-dsRed). The Au-dsRed complex is prepared by place exchange[41−44] of the BSPP passivant on the AuNP with the *S*-dsRed gene in a 1/1.1 gene/AuNP mole ratio for 48 h in sparged TBS buffer (pH = 7.4). To accomplish the place exchange reaction, the gene mixture is resuspended in TBS buffer (pH 7.4), the dithiol protecting group at the 5′ end of the gene is cleaved by treatment with 20 mM dithiothreitol (DTT) for 2h at RT, and the product is purified by a NAP-5 (Sephadex G-25 DNA grade) gravity flow size exclusion column to remove excess DTT, the thiol protecting group, and excess synthetic DNA. The activated thiol functionalized gene is used immediately to prevent disulfide formation. The 6 nm AuNP is resuspended in TBS buffer, added to the gene, and allowed to mix on a rotisserie at RT for 48 h. The Au-dsRed is pelleted out of the reaction mixture by centrifugation at 3000 rpm allowing removal of unbound gene and excess 6 nm AuNP from the reaction. Gel electrophoresis (1% agarose) exhibits a single band confirming formation of the Au-dsRed construct and lack of free AuNP in the isolated product (Supplemental Figure SF2). Further analysis of the samples was conducted by absorption spectroscopy analysis of the DNA and Au SPR UV−vis features.

Preparation of the Au-siRNA Complex. The Au-siRNA complex is prepared by place exchange of the BSPP passivant on the AuNP with a 5′ C_6 free thiol (on sense strand) ds-siRNA (19 bp) in a 50/1 siRNA/AuNP mole ratio for 48 h in sparged TBS buffer (pH = 7.4) at 4 °C, following standard protocols previously employed by our group.[44] The sense strand is 5′-HS-CUA CCU GUU CCA UGG CCA Att-3′, and the antisense strand is 3′-GAU GGA CAA GGU ACC GGU U-5′. The ds-siRNA sequence is annealed at 60 °C in TBS buffer in a 1:1 sense/antisense ratio following standard methods and verified by gel electrophoresis (10% PAGE). The formation of the free thiol on the 3′ end of the antisense strand is accomplished by treatment of the annealed ds-siRNA sequence with 20 mM DTT for 2 h at RT, purification on a NAP-5 (Sephadex G-25 DNA grade) gravity flow size exclusion column to remove excess reactants, and immediate use to eliminate disulfide formation. The Au-siRNA complex is isolated by addition of sodium chloride to induce precipitation of the complex, followed by centrifugation at 3000 rpm. The complex is purified on a NAP-5 column to remove unreacted siRNA.

Preparation of the Au-dsRed/siRNA Complex. The Au-dsRed/siRNA complex is prepared by resuspending Au-dsRed in TBS buffer and addition of the ds-siRNA in a 50:1 ratio. The place exchange reaction is allowed to proceed at 4 °C for 24 h. The final Au-dsRed/siRNA complex is isolated from the TBS buffer by centrifugation at 3000 rpm without the addition of sodium chloride, and is washed with ethanol. The Au-dsRed/siRNA complex is validated by absorption spectroscopy. Gel electrophoresis was not utilized in the analysis of the Au-dsRed/siRNA complex, as the gel cannot distinguish between the Au-dsRed and the Au-dsRed/siRNA complex.

Analysis of AuNP Complexes. The hydrodynamic radius of the Au-complexes and biochemical controls were analyzed using dynamic light scattering (DLS, Supplemental Figure SF4). DLS is performed on a DynaPro Titan DLS system (Wyatt Technologies, Santa Barbara) at 20% laser power (830 nm) for complexes resuspended in DI water. The hydrodynamic radius is calculated by averaging 20 measurements with an acquisition time of 1 s. The ratio of DNA to siRNA to AuNP is extracted by a Beer−Lambert law analysis using UV−vis spectroscopy (Supporting Figure SF1C). In addition, the Au-complexes were analyzed by treatment a 2 mM sodium cyanide to dissolve the gold (5 μM) from the dye-labeled DNA or siRNA. The DNA or siRNA were labeled in individual experiments and after treatment, and fluorescein absorbance or emission was used to determine concentration of the DNA and siRNA on the surface of the AuNP (Supplemental Figure SF5).

Cell Culture Transfection and Analysis. Cell transfection studies are carried out in CRL-2794 (ATCC), a cell line derived from the human embryonic kidney line (HEK)-293 to expresses an unstable form of green fluorescent protein (GFP) with a half-life of the protein of ∼30 min. The CRL-2794 cells are plated with a density of 30 000/cm^2 and cultured at 37 °C with 5% CO_2 in Dulbecco's Modified Eagle's Medium (DMEM-5523) (Sigma) supplemented with addition of 10% cosmic calf serum (Hyclone) and 10% nonessential amino acid mix (Sigma). Transfection is carried out 24 h after plating by media exchange to OptiMEM and treatment with cell lines, with the 4 μg Au-complexes encapsulated in 10 μL Lipofectamine2000 (Invitrogen), according to the optimization protocol offered by the manufacturer. The ratio of Lipofectamine 2000 to the Au-complex was based on viability (trypan blue, not shown) to ensure minimal toxicity (>95% viability) 24 h post transfection. The transfection is allowed to proceed for 4 h, media exchanged to supplemented DMEM-5523, and the cells were analyzed 20 h later. The cell viability following transfection was >95% versus control by analysis of the Trypan blue exclusion test. Transfection efficiency of the siRNA and the dsRed gene is analyzed by optical microscopy and flow cytometry.

Protein Expression Analysis. Evaluation of the siRNA knock down and gene transfection yields will be assayed by monitoring the fluorescent signature for the fluorescent proteins (endogenous GFPu, and exogenous dsRed) providing an experimental handle for quantitative analysis of the expression level of GFPu in CRL-2794 and the induced expression of dsRed following AuNP-complex delivery. The fluorescent signature in the CRL-2794 cells is analyzed qualitatively by live cell imaging using spectral confocal microscopy (Nikon TE-2000 E2 eclipse C-1si) and quantitatively by flow cytometry on 10 000 events acquired on a BD FACS Canto II with 488 nm excitation and detection of GFPu using the FITC filter set (530/15) and dsRed PE-A (585/42) filter set. In flow cytometry, the statistics were determined as reference to the parent population in each set of studies. The confocal laser scanning microscope (CLSM) is equipped with a Nikon CFI Plan Apochromat TIRF 60× oil immersion objective (Numerical Aperture (NA) 1.49, 0.12 mm working distance (WD)) with a 5.75 electronic zoom to fill Nyquest sampling in addition to a CFI Plan Apochromat 40× objective (NA 0.95, 0.14 mm WD), 5.49 electronic zoom. The samples are imaged with a Cool SNAP HQ2 monochrome camera (Photometric), and analyzed with Nikon NIS Elements software. Each Au-complex and control data set is collected in triplicate.

RESULTS AND DISCUSSION

Engineering the AuNP Bimodal Agent. The design of the bimodal AuNP agent for controlling endogenous GFP knockdown and inducing exogenous dsRed turn-on within CRL-2794 is shown in Figure 1. The bimodal agent is constructed by sequentially place-exchanging onto a 6 nm AuNP surface a 5′-C_6 thiol modified full gene to induce dsRed expression and a 5′-C_6 thiol modified (sense) siRNA to knock-down GFPu expression.[45] The construct is achieved by first covalently appending the gene to the AuNP surface followed by attachment of the siRNA. The approach is analogous to backfilling of a second thiol following stamp patterning in self-assembled monolayers on Au films. Coordination of the thiol functional group to the AuNP is accomplished by displacement of the BSPP phosphine passivating layer on the AuNP. Place exchange reactions have been shown to be effective at

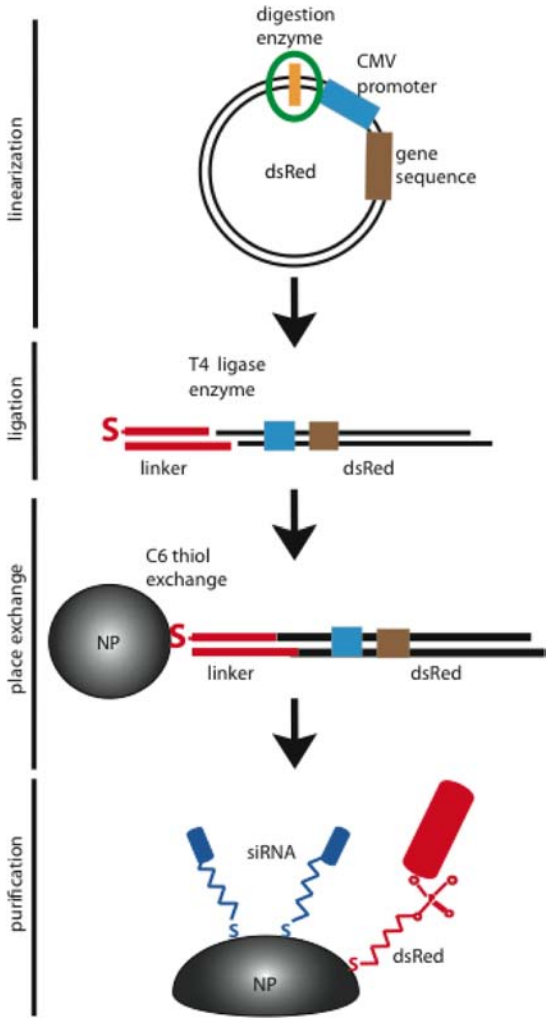

Figure 1. Schematic of coassembly on the surface of a AuNP. DsRed is linearized with AflIII, followed by a ligation to a ds-linker strand with a C6 thiol moiety at the 5′ end. The thiol is reduced and appended to the AuNP followed by a back-loading of siRNA.

formation of a Au-thiol bond for appending DNA and RNA in previous studies.[43,44]

A thiol modified dsRed gene is prepared by cutting a bacterial plasmid with AflIII, a sequence specific digestion enzyme, to linearize the gene and produce a sticky finger overhang for ligation of a synthetic ds-DNA linker containing the 5′ terminal thiol moiety. Ligation of the synthetic linker to the linearized gene is accomplished by use of T4 ligase. The place exchange reaction for the gene results in the appendage of approximately one gene per AuNP reflecting the 1:1.1 stoichiometric reaction ratio. The siRNA is backfilled onto the AuNP surface using a 150:1 siRNA to AuNP ratio to displace the remaining BSPP form the AuNP surface. The gene to siRNA loading ratio will be a stochastic distribution, although earlier studies in RNA and DNA loading onto AuNP surfaces have shown near stoichiometric control is achievable.[46]

The rationale of the design in Figure 1 reflects the desire to deliver siRNA and a gene that are fully functional into a cell. The nanoparticle concentration is limited by toxicity issues related to lipofectamine and gene toxicity, which arise at high concentrations of delivered gene or lipofectamine. To assess cytoxicity, a toxicity assay using trypan blue was carried out on the AuNP-gene constructs between 0 and 2.0 $\mu g/cm^2$ in CRL-2794 (Supplemental Figure SF3). The concentration dependent toxicity of AuNP-gene was analyzed at 12, 24, and 48 h. The experimental data shows increased toxicity for samples >0.4 $\mu g/cm^2$, and therefore, we carried out all studies below the toxicity threshold. The AuNP-gene/siRNA ratio is chosen to maximize the delivered siRNA to gene into the cell. It is known siRNA is less stable in the endosome than a full gene due to nuclease sensitivity.[47]

To interpret the ratio of gene and siRNA to the nanoparticle, an assumption is made that the gene will dominate mobility in the gel, the DLS size, and the absorption spectra due to the larger extinction coefficient (~250× larger) for the gene relative to the siRNA. The use of a single gene labeling approach allows characterization of the sample due to the ability to isolate the construct as a single band in gel electrophoresis (Supplemental Figure SF2). The remaining sites on the AuNP surface are back-loaded by siRNA by using an excess of siRNA to displace the remaining BSPP via thermodynamics. Early place exchange reactions on AuNPs with peptides and proteins have shown complete displacement of the BSPP.[42,48] Comparison of the AuNP-gene/siRNA assembly to a control electrostatic assembly where the gene is nonspecifically (no synthetic C_6 linker) assembled onto the AuNP results in a smeared band for the AuNP due to dissociation of the gene from the Au surface as the gel elutes. The smeared band for the control reflects the lower stability of the noncoordinated species supporting the picture of a covalent thiol−Au coupling of the gene to the AuNP surface.

The shift in the size and autocorrelation function for the DLS can distinguish between a bound gene and the free gene (Supplemental Figure SF4). A ~1:1 loading ratio of the gene onto the AuNP reflecting the reaction stoichiometry can be confirmed by inspection of dynamic light scattering (DLS) data. The shift in the size and autocorrelation function for the DLS can distinguish between a bound gene and the free gene. The globular gene has a DLS size of 171.4 nm. Upon binding of the gene to the NP, the DLS data shifts to 227 nm from 23 nm for the 6 nm AuNP. The DLS data is typically larger than the nanoparticle size when measured by DLS. Mattoussi et al. observed ~20 nm for a 6 nm AuNP consistent with our measurement.[49,50] The size difference of $\Delta \sim 56$ can be interpreted as supporting the one gene per AuNP model. The shift is larger than expected but within the expected error based upon the repackaging of the globular gene once bound. If two were bound, we would expect a value that is twice the diameter of the single gene. If a distribution of gene assembly had occurred we would lose the correlation. The tight autocorrelation function and a single band in the gel electrophoresis supports that a single gene has bound the nanoparticle.

Analyzing the likelihood of binding versus pure electrostatics can also be measured by DLS experiments. The hydrodynamic radius for the series of Au-bio agents (Au-dsRed, Au-dsRed/siRNA) and nonspecific assemblies was extracted from the DLS autocorrelation function, shown in Supplemental Figure SF4, assuming a globular conformation. The DLS data reveals that the hydrodynamic radii for the thiol coordinated versus nonspecific assembly for the Au-dsRed in deionized water is 227 nm (coordinated) versus 184 nm (nonspecific), and for the Au-dsRed/siRNA it is 200 nm (coordinated) versus 142 nm (nonspecific). The AuNP with the BSPP has a hydrodynamic radius of 13 nm, while the globular uncoordinated gene exhibits a radius of 171 nm. The DLS data for the electrostatic versus

dx.doi.org/10.1021/ja307502x | J. Am. Chem. Soc. 2012, 134, 19722−19730

the assembled structures taken together supports a model where a covalent coupling exists between the AuNP and the appended bioagents.

The observation of a reduced dimension in the DLS data for the nonspecific complex may reflect contributions from nonglobular confirmations in the coordinated AuNP bioagent or a decrease in secondary packaging due to increased conformational rigidity when assembled at the AuNP surface. The nature of the secondary interactions for the nonspecifically assembled bioagents can include interactions of the phosphate backbone with the AuNP surface, electrostatic packaging, and entropic and enthalpic packing interactions. The nonspecific interactions are likely to be affected by changes in the ionic strength of the media, while the covalently linked bioagents are less likely to be influenced. The effect of added NaCl (150 mM) to the samples yields changes in the measured hydrodynamic radius for Au-dsRed of Δ = +9 nm (coordinated) versus −3 nm (nonspecific) and Au-dsRed/siRNA is Δ = 0 nm (coordinated) versus +52 nm (nonspecific). The globular gene changes from 202 to 208 nm in the presence of 150 mM NaCl. With the exception of the nonspecific gene on the Au-siRNA NP, the AuNP complex exhibits insignificant changes in hydrodynamic radii suggesting electrostatic interactions are not the dominant mechanism for packaging. The observed change in hydrodynamic radius is consistent with expectations for changes in packaging of the globular gene with increased salt concentration.

The DLS data supports a single gene is bound to the AuNP surface, as a clear shift in the DLS spectra was observed that can be accounted for by the addition of a single gene to the AuNP-siRNA. The experimental data is inconsistent with the binding of two or more genes. The siRNA to gene ratio cannot be accurately assessed by the DLS results. The gel electrophoresis data and the DLS data allow absorption data to provide a semiquantitative estimate of the DNA to siRNA ratio in the AuNP-gene/siRNA bimodal agent. By inspection of the UV−vis absorption spectra for the bimodal complex in comparison to controls (Supplemental Figure SF1C), it is clear that the AuNP has a well-defined LSPR plasmon absorption at 525 nm. The gene and siRNA absorb at 260 nm, while the BSPP has an absorption peak at 275 nm. Although the spectra overlap, the absorption data can be analyzed if we assume one gene per AuNP and all the BSPP has been place exchanged by the siRNA, as previously observed in protein exchange studies.[42]

Analysis of intensity of the AuNP with an appended gene but not back loaded with the siRNA confirms the DLS data of a 1:1 loading ratio of the gene to AuNP. The analysis is made using the localized surface plasmon ($\varepsilon_{525\text{nm(LSPR)}} \sim 2 \times 10^7$ L mol^{-1} cm^{-1}) at 525 nm versus the gene absorption at 260 nm ($\varepsilon_{260\text{(gene)}} \sim 1 \times 10^9$ L mol^{-1} cm^{-1}). It is assumed that the contribution of the BSPP ($\varepsilon_{260\text{(BSPP)}} = 1.7 \times 10^2$ L mol^{-1} cm^{-1}) and AuNP-BSPP ($\varepsilon_{260\text{(AuNP)}} = 2.7 \times 10^7$ L mol^{-1} cm^{-1}) to the 260 nm absorption for the gene is negligible due to the 100× greater extinction coefficient for the gene. The contribution of BSPP at 260 nm is insignificant as shown in the absorption data. Using the Beer−Lambert law to analyze the concentration of the gene to AuNP yields a mole ratio of 1.06 gene to AuNP, consistent with the DLS data of 1:1 ratio for gene to AuNP. The Beer−Lambert law calculation was corrected for the absorption of the AuNP-BSPP at 260 nm.

To analyze the siRNA loading ratio, the change in the optical absorption at 260 nm following siRNA back-loading was measured. The siRNA has an extinction coefficient of $\varepsilon_{260} \sim 3.4 \times 10^5$. The measured increase in intensity in the 260 nm absorption intensity relative to the AuNP gene construct is consistent with siRNA loading of ∼50 to 1 AuNP, when corrected for the AuNP absorption contribution at 260 nm. The calculated ratio is an ensemble averaged value and reflects a stochastic distribution.

In the Supporting Information (Supporting Figure SF5), the Beer−Lambert law analysis for the siRNA to AuNP loading ratio was further confirmed using a fluorescein labeled synthetic sequence. We have utilized dye labeled siRNA to measure loading ratios in nanometal surface energy transfer (NSET) molecular beacon studies in our group.[44] In the absorption data, the fluorescein absorption can be seen at 500 nm as a distinct feature in the shoulder of the LSPR band. Comparison of the LSPR intensity to the fluorescein absorption value using appropriate extinction coefficients yields a mole ratio value of 56:1, providing strong support of the siRNA to AuNP ratio measured by the Beer−Lambert law analysis.

Evidence that the siRNA is bound to the NP can be gained by inspection of the fluorescein emission experiment in Supporting Figure SF5. No fluorescein emission is observed when bound to the AuNP as expected from a nanometal surface energy transfer molecular beacon.[51,52] The release of the siRNA by dissolving the AuNP through addition of 2 mM NaCN confirms the siRNA is appended to the nanoparticle. The combined experimental data for the bimodal agent supports a model where a covalent appendage attaches one gene per AuNP with a 1:50 ratio of gene to siRNA.

Protein Expression. The time dependent change in the exogenous (dsRed) and endogenous (GFPu) protein expression in CRL-2794 was analyzed by transfection of the bioagents (Au-dsRed, Au-dsRed/siRNA), their nonspecific analogues, and the linearized gene and siRNA using lipofectamine2000 at 30% confluence (30 000cells/cm^2) in 6-well plates at a concentration of 0.4 mg/cm^2 in cells, to maintain >95% cell viability throughout the experiment. The CRL-2794 cell line was chosen due to the native expression of an ubiquitinated GFP (GFPu) having a half-life of approximately 30 min, determined by Kopito et al., by pulse chase analysis,[53] allowing the change in intracellular GFP to be directly detectable on the time scale of the experiment. Normal GFP has a half-life of 24 h,[54] which would limit the ability of accurately analyzing gene knockdown.

The time scale of the protein analysis experiment was chosen from analyzing the timing of gene release and gene expression by optical microscopy monitoring of the event. The protein expression can be visualized in the microscope directly, while release of the nucleic acid agents requires the use of a molecular beacon. The use of a nanometal surface energy transfer molecular beacon[51,52] study allows the release to be visualized by appending a fluorescein (FAM) to the linker strand 15bp from the AuNP surface. The FAM is proximally quenched by the AuNP via a nanometal surface energy transfer (NSET) mechanism when the gene is bound.[51,52] Upon release the dye emits immediately resulting in a "flash" molecular beacon in the endosome. In the Supporting Information (SF5), the data shows the release of the gene from the AuNP surface as evidenced by the appearance of a green fluorescence signature for FAM within the endosome at 12 h. The gene expression is signaled by the appearance of the dsRed fluorescence (12 h). The appearance of both signals at 12 h does not indicate the process has occurred simultaneously as the timing of the event and half-life of the dsRed folding versus release from the AuNP

are not on the same time scale. The release of the gene from the AuNP to the point of expression indicates the time needed for maximal expression of the gene, after escape from the endosome (Supplemental Figure SF6). On the basis of the optical microscopy imaging, the flow cytometry time points of 24, 48, and 72 h were chosen to optimize data collection.

Figure 2 shows the optical microscopy images 24 h after cell transfection by the gene, the Au-dsRed, and the Au-siRNA/

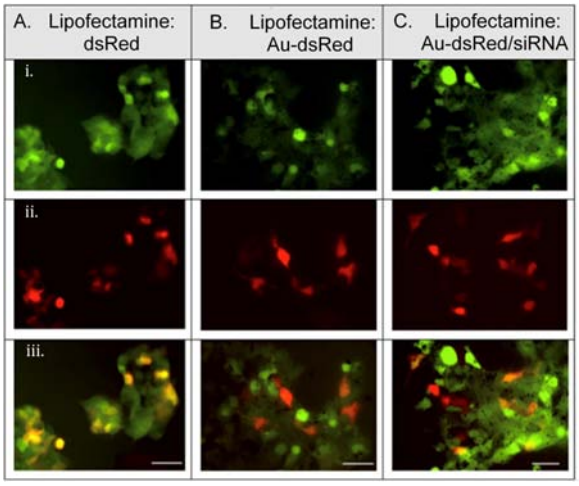

Figure 2. Wide-field optical images of CRL-2794 cells at 24 h following transfection with (A) lipofectamine:dsRed, (B) lipofectamine:Au:-dsRed, and (C) lipofectamine:Au:dsRed/siRNA. The wide-field images are shown for the (i) green (528−553 nm) corresponding to GFPu, (ii) red (578−633 nm) corresponding to dsRed, and (iii) red/green overlay for GFPu and dsRed. Scale bar is 50 μm.

dsRed. The optical images comparing the green channel (emission bandpass 528−553 nm), the red channel (emission bandpass 578−633 nm), and the red/green overlay clearly show the presence of the endogenous GFPu (Figure 2i) in the green and green/red overlay (Figure 2iii), while exogenous dsRed expression is observed in the red (Figure 2ii) and red/green overlay (Figure 2iii), respectively. A plot of the red and green intensity versus trajectory for a single cell confirms the presence of the AuNPs in the endosomes when compared to images of the CRL-2794 control cells (Figure 3). In Figures 2 and 3, the AuNP is observable as "black" spots where the GFP emission is not observed in the green channel due to an inner filter effect for the Au LSPR band. The "black" spots do not appear in the absence of the AuNPs in the cells. Analysis of the AuNP transfection indicates 65% of the cells are transfected at 24 h following treatment.

The level of exogenous and endogenous expression for each of the agents at 24 h is roughly equivalent in the micrographs, but statistically meaningless due to the effects of depth of field and focal plane aberrations to the observed intensity in the image. Statistically relevant expression levels for GFPu and dsRed expression were obtained from flow cytometry analysis of 10 000 cell events carried out at 24, 48, and 72 h post transfection (Figure 4, Supplemental Figure SF7). The flow cytometry data in Figure 4 reveals the endogenous and exogenous protein expression is impacted by the AuNP bioagent treatment. Treatment of the CRL-2794 cells by Au-siRNA/dsRed results in knockdown of GFP by 20% within 24 h and is observed for 48 h. The initiation of dsRed expression occurs during the same time frame but exhibits a continued

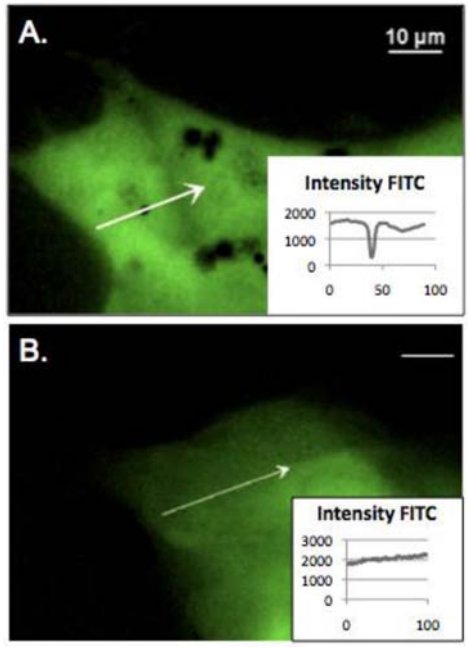

Figure 3. Wide field optical image in the green channel showing the presence of a dark spot due to the inner filter effect for the AuNP and a plot of the GFPu intensity along the arrow in the micrographs for (A) AuNP-siRNA/dsRed transfected CRL-2794 cells at 24h compared to the (B) lipofectamine control cells. Scale bar is 10 μm.

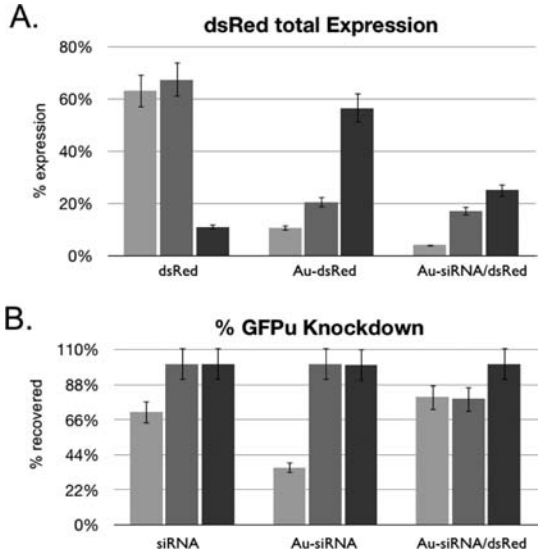

Figure 4. Time dependent flow cytometry data (10 000 events) for CRL-2794 cells transfected at 0.4 μg/cm^2 in cells. The flow cytometry data is collected at 24 h (light), 48 h (medium), and 72 h (dark) post transfection: (A) dsRed expression for linearized dsRed gene (gene), Au-dsRed, and Au-siRNA/dsRed; and (B) GFPu knockdown in siRNA, Au-siRNA, Au-siRNA/dsRed.

increase in expression over the course of the 72 h experiment. The Au-siRNA sequence exhibits 65% knockdown at 24 h and recovers to pretreatment levels within 48 h, while siRNA alone shows 30% knockdown over the same time period (Figure 4). The statistics were determined by comparing the parent populations of the controls determined in each study using flow cytometry.

dx.doi.org/10.1021/ja307502x | J. Am. Chem. Soc. 2012, 134, 19722−19730

The initiation of knockdown of GFP is similar for the AuNP agents and the native siRNA sequence, but the length of effect is significantly longer for the AuNP delivered siRNA with knockdown occurring for 48 h before the cells recover to normal GFP expression levels. The total knockdown is highest for the Au-siRNA, followed by Au-dsRed/siRNA and finally the native siRNA. The higher magnitude of knockdown for the Au-siRNA versus the Au-dsRed/siRNA is believed to reflect the loading ratio of siRNA, while the decreased knockdown for the native siRNA may reflect reduced siRNA delivery into the cell, siRNA endosomal degradation, knockdown occurring faster than experimentally measured,[55] or improved functionality of the AuNP complexed siRNA due to protective attributes associated with siRNA coordination to the AuNP surface, as previously suggested.[33] When the AuNP complex was not in the presence of a transfection reagent, or the transfection reagent alone, or when the transfection reagent and AuNP were used, no effect on GFP expression level was observed.

The flow cytometry data for dsRed expression reveals the highest expression level is observed at 72 h for Au-dsRed and Au-dsRed/siRNA. The gene induced exogenous expression of dsRed is longer lasting but delayed for the AuNP agents when compared to a linearized plasmid delivered in lipofectamine2000. The dsRed linearized gene shows the highest overall expression level, but does the shortest time frame for expression. The AuNP based transfection strategy results in dsRed expression after 72 h in the CRL-2794 cells for the Au-dsRed of 56% and Au-dsRed/siRNA of 25% relative to the <10% expression remaining for transfection by the gene alone. The improved expression level is intriguing and may suggest either more efficient endosomal escape of the gene or improved protection of the gene from degradation leading to a higher number of intact genes delivered into the cytosol.

The surprising result of similar time scale for effects on protein expression for the delivered siRNA and gene are believed to reflect a delay of siRNA escape from the AuNP surface due to the unpackaging of siRNA requiring the initial release of the gene from the NP surface due to packaging of the larger gene around the NP circumference, effectively embedding the siRNA. The delay in siRNA release would delay the onset of knockdown, consistent with the timing observed in Figure 2.

Evidence of Formation of a Stable Rransform. The increasing dsRed levels out to 72 h within the CRL-2794 cells, but short-term knockdown of GFPu (48 h) following transfection with the AuNP bioagent is consistent with the anticipated differences in the mechanism for protein regulation. siRNA is a transient agent degraded intracellularly following formation of the RISC complex, while the gene is transcribed to mRNA and is not necessarily degraded. Since the GFP expressed by the CRL-2794 cell is modified by an ubiquitin tag, the GFP is rapidly degraded by the cell resulting in a 30 min half-life. The dsRed on the other hand is not degraded by the cell, has a half-life of >24 h, and therefore will be observed to build up during the experimental time scale ad may continue to increase if gene insertion into the genome occurs. On the other hand, it is anticipated that the dsRed expression level per cell will decrease as the cells divide if the delivered gene is degraded and does not lead to gene insertion.

Image analysis of optical plates for cells cultured for 25 days following transfection indicate dsRed expression continues to increase with 34% of the CRL-2794 expressing dsRed following treatment by Au-dsRed (Figure 5A). Cells transfected by the dsRed gene without the AuNP at 25 days exhibits negligible dsRed expression. The higher level and longer time frame of expression observed in the cell population treated with the AuNP agent implies that a more efficient transfection and stable gene insertion has occurred. To test the hypothesis, the dsRed expressing CRL-2794 cells were sorted and cultured for 91 days. Culturing the selected cells results in a stable colony being isolated as shown in Figure 5B. Western blot analysis of nine separate colonies shows dsRed expression levels are nearly identical.

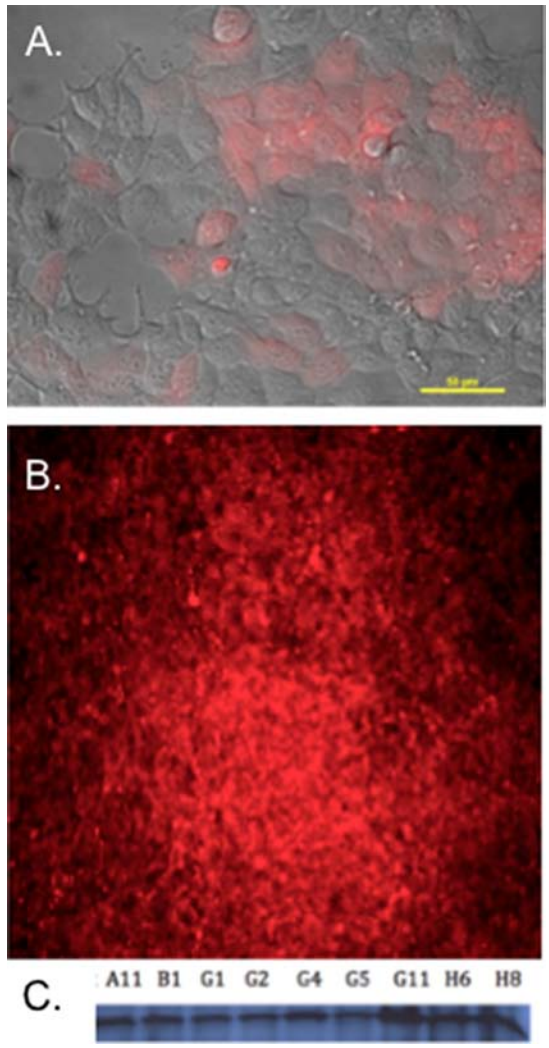

Figure 5. (A) Wide field optical image of Au-dsRed transfected cells at 25 days. (B) Colony expression and (C) western blot of dsRed expression results on nine separate colonies for sorted cells CRL-2794 cells after 3 months.

The observed ease in which a stable transform can be generated by transfection with the AuNP agents is intriguing. Typically the efficiency of transfection of a gene leading to a stable transform is less than 1% and requires antibiotic sorting, and the time scale for obtaining a stable transform can be as long as 3 months. Observation of stable transforms within such a short time frame strongly suggests that the use of the AuNP as a nonviral transfection vector can allow single passage transfection of cells without the requirement for antibiotic sorting or multiple transfection steps.

CONCLUSION

Whether the goal is transgenic animals or selectively engineered cultured cell lines for biomedical research, the ability to reproducibly incorporate a desirable genetic code into a selected genome represents a global goal in genetic engineering. The AuNP bioagents demonstrate extended siRNA knockdown of endogenous protein expression and initiation of exogenous protein expression on similar time scales can be achieved through cofunctionalization on the surface of a AuNP. The level of knockdown and induced expression occurs to a higher level and longer duration than transfection using the raw siRNA or linearized gene. The AuNP agent is easily modifiable, and demonstrates potential for downstream application studies where long-term gene expression therapies are needed. The results clearly demonstrate formation of stable colonies within weeks of treatment without excessive cell manipulation. The ability to manipulate exogenous and endogenous protein populations within a cell on similar time scale is potentially transformative for cell therapeutics and may offer a routine cell transfection. This nonviral gene-delivery strategy introduces a dual-labeled, nanoparticle-mediated platform for simultaneous delivery of multiple gene products on a single nanomaterial surface. Further efforts include specific cell targeting, effect of varying nucleic acid stoichiometries, and linearized plasmid delivery of disease-related proteins as potential gene therapeutic candidates are underway.

ASSOCIATED CONTENT

Supporting Information

AuNP construct characterization data including TEM, gel electrophoresis, extinction spectra, fluorescence data, toxicity, and dynamic light scattering. Flow cytometry results for dsRed and GFPu levels in the CRL-2794 cells. This material is available free of charge via the Internet at http://pubs.acs.org.

AUTHOR INFORMATION

Corresponding Author

strouse@chem.fsu.edu

Present Address

[†]U.S. Army Research Laboratory, Sensors and Electron Devices, Adelphi, MD 20783−1197.

Notes

The authors declare no competing financial interest.

ACKNOWLEDGMENTS

We wish to acknowledge the National Science Foundation under CHE-0911080 for support of the research.

We wish to acknowledge Joan Hare, Ph.D., for assistance in cell culture techniques, and Claudius Mundoma, Ph.D., for experimental assistance in dynamic light scattering at the Institute for Molecular Biophysics. In addition, we wish to thank Ruth Didier for assistance in flow cytometry at the College of Medicine.

REFERENCES

(1) Chen, A. A.; Derfus, A. M.; Khetani, S. R.; Bhatia, S. N. *Nucleic Acids Res.* **2005**, *33*, e190.
(2) Duran, M. C.; Willenbrock, S.; Barchanski, A.; Muller, J. M.; Maiolini, A.; Soller, J. T.; Barcikowski, S.; Nolte, I.; Feige, K.; Murua Escobar, H. *J. Nanotechnol.* **2011**, *9*, 47.
(3) Giljohann, D.; Seferos, D.; Prigodich, A.; Patel, P.; Mirkin, C. *J. Am. Chem. Soc.* **2009**, *131*, 2072.
(4) Gomes-da-Silva, L. C.; Fonseca, N. A.; Moura, V.; Pedroso de Lima, M. C.; Simões, S.; Moreira, J. N. *Acc. Chem. Res.* **2012**, *45*, 1163.
(5) Huang, C.; Li, M.; Chen, C.; Yao, Q. *Expert Opin. Ther. Targets* **2008**, *12*, 637.
(6) Kawakami, S.; Higuchi, Y.; Hashida, M. *J. Pharm. Sci.* **2008**, *97*, 726.
(7) Probst, C. E.; Zrazhevskiy, P.; Bagalkot, V.; Gao, X. *Adv. Drug. Delivery Rev.* **2012**, DOI: 10.1016/j.addr.2012.09.036.
(8) Rosi, N. L.; Giljohann, D. A.; Thaxton, C. S.; Lytton-Jean, A. K.; Han, M. S.; Mirkin, C. A. *Science* **2006**, *312*, 1027.
(9) Gavrilov, K.; Saltzman, W. M. *Yale J. Biol. Med.* **2012**, *85*, 187.
(10) Ali, H. M.; Urbinati, G.; Raouane, M.; Massaad-Massade, L. *Expert Rev. Clin. Pharmacol.* **2012**, *5*, 403.
(11) Samakoglu, S.; Lisowski, L.; Budak-Alpdogan, T.; Usachenko, Y.; Acuto, S.; Di Marzo, R.; Maggio, A.; Zhu, P.; Tisdale, J. F.; Riviere, I.; Sadelain, M. *Nat. Biotechnol.* **2006**, *24*, 89.
(12) Amaral, M. D. *J. Inherited Metab. Dis.* **2006**, *29*, 477.
(13) Atkinson, H.; Chalmers, R. *Genetica* **2010**, *138*, 485.
(14) Nayak, S.; Herzog, R. W. *Gene Ther.* **2010**, *17*, 295.
(15) Daya, S.; Berns, K. I. *Clin. Microbiol. Rev.* **2008**, *21*, 583.
(16) Reischl, D.; Zimmer, A. *Nanomed. Nanotechnol. Biol., Med.* **2009**, *5*, 8.
(17) Flanagan, M.; Gimble, J. M.; Yu, G.; Wu, X.; Xia, X.; Hu, J.; Yao, S.; Li, S. *Cancer Gene Ther.* **2011**, *18*, 579.
(18) Al-Dosari, M. S.; Gao, X. *AAPS J.* **2009**, *11*, 671.
(19) Coura Rdos, S.; Nardi, N. B. *Virol. J* **2007**, *4*, 99.
(20) Coura, R. D.; Nardi, N. B. *Genet. Mol. Biol.* **2008**, *31*, 1.
(21) Sakurai, H.; Kawabata, K.; Sakurai, F.; Nakagawa, S.; Mizuguchi, H. *Int. J. Pharm.* **2008**, *354*, 9.
(22) Wang, Y.; Gao, S.; Ye, W. H.; Yoon, H. S.; Yang, Y. Y. *Nat. Mater.* **2006**, *5*, 791.
(23) Malam, Y.; Loizidou, M.; Seifalian, A. M. *Trends Pharmacol. Sci.* **2009**, *30*, 592.
(24) Wijaya, A.; Schaffer, S. B.; Pallares, I. G.; Hamad-Schifferli, K. *ACS Nano* **2009**, *3*, 80.
(25) Song, S.; Liang, Z.; Zhang, J.; Wang, L.; Li, G.; Fan, C. *Angew. Chem., Int. Ed.* **2009**, *48*, 8670.
(26) Lytton-Jean, A. K.; Mirkin, C. A. *J. Am. Chem. Soc.* **2005**, *127*, 12754.
(27) Sandhu, K. K.; McIntosh, C. M.; Simard, J. M.; Smith, S. W.; Rotello, V. M. *Bioconjugate Chem.* **2002**, *13*, 3.
(28) Giljohann, D. A.; Seferos, D. S.; Patel, P. C.; Millstone, J. E.; Rosi, N. L.; Mirkin, C. A. *Nano Lett.* **2007**, *7*, 3818.
(29) Kim, S. T.; Chompoosor, A.; Yeh, Y. C.; Agasti, S. S.; Solfiell, D. J.; Rotello, V. M. *Small* **2012**, *8*, 3253.
(30) Braun, G. B.; Pallaoro, A.; Wu, G.; Missirlis, D.; Zasadzinski, J. A.; Tirrell, M.; Reich, N. O. *ACS Nano* **2009**, *3*, 2007.
(31) Yezhelyev, M. V.; Qi, L.; O'Regan, R. M.; Nie, S.; Gao, X. *J. Am. Chem. Soc.* **2008**, *130*, 9006.
(32) Elbakry, A.; Zaky, A.; Liebl, R.; Rachel, R.; Goepferich, A.; Breunig, M. *Nano Lett.* **2009**, *9*, 2059.
(33) Giljohann, D. A.; Seferos, D. S.; Prigodich, A. E.; Patel, P. C.; Mirkin, C. A. *J. Am. Chem. Soc.* **2009**, *131*, 2072.
(34) Lytton-Jean, A. K.; Langer, R.; Anderson, D. G. *Small* **2011**, *7*, 1932.
(35) Ghosh, P. S.; Kim, C. K.; Han, G.; Forbes, N. S.; Rotello, V. M. *ACS Nano* **2008**, *2*, 2213.
(36) Mirkin, C. A.; Letsinger, R. L.; Mucic, R. C.; Storhoff, J. J. *Nature* **1996**, *382*, 607.
(37) Pissuwan, D.; Niidome, T.; Cortie, M. B. *J. Controlled Release* **2011**, *149*, 65.
(38) Salem, A. K.; Searson, P. C.; Leong, K. W. *Nat. Mater.* **2003**, *2*, 668.
(39) Duncan, B.; Kim, C.; Rotello, V. M. *J. Controlled Release* **2010**, *148*, 122.
(40) Frens, G. *Nature, Phys. Sci.* **1973**, *241*, 20.
(41) Singh, M. P.; Strouse, G. F. *J. Am. Chem. Soc.* **2010**, *132*, 9383.
(42) Kogot, J. M.; Parker, A. M.; Lee, J.; Blaber, M.; Strouse, G. F.; Logan, T. M. *Bioconjugate Chem.* **2009**, *20*, 2106.

(43) Jennings, T.; Strouse, G. *Adv. Exp. Med. Biol.* **2007**, *620*, 34.
(44) Jennings, T. L.; Schlatterer, J. C.; Singh, M. P.; Greenbaum, N. L.; Strouse, G. F. *Nano Lett.* **2006**, *6*, 1318.
(45) Dreaden, E. C.; Alkilany, A. M.; Huang, X.; Murphy, C. J.; El-Sayed, M. A. *Chem. Soc. Rev.* **2012**, *41*, 2740.
(46) Hurst, S. J.; Lytton-Jean, A. K.; Mirkin, C. A. *Anal. Chem.* **2006**, *78*, 8313.
(47) Tseng, Y.; Mozumdar, S.; Huang, L. *Adv Drug Deliv Rev* **2009**, *61*, 721.
(48) Kogot, J. M.; England, H. J.; Strouse, G. F.; Logan, T. M. *J. Am. Chem. Soc.* **2008**, *130*, 16156.
(49) Oh, E.; Susumu, K.; Goswami, R.; Mattoussi, H. *Langmuir* **2010**, *26*, 7604.
(50) Pons, T.; Medintz, I. L.; Sapsford, K. E.; Higashiya, S.; Grimes, A. F.; English, D. S.; Mattoussi, H. *Nano Lett.* **2007**, *7*, 3157.
(51) Jennings, T. L.; Singh, M. P.; Strouse, G. F. *J. Am. Chem. Soc.* **2006**, *128*, 5462.
(52) Yun, C. S.; Javier, A.; Jennings, T.; Fisher, M.; Hira, S.; Peterson, S.; Hopkins, B.; Reich, N. O.; Strouse, G. F. *J. Am. Chem. Soc.* **2005**, *127*, 3115.
(53) Bence, N. F.; Sampat, R. M.; Kopito, R. R. *Science* **2001**, *292*, 1552.
(54) Corish, P.; Tyler-Smith, C. *Protein Eng.* **1999**, *12*, 1035.
(55) Wang, J.; Lu, Z.; Wientjes, M. G.; Au, J. L. *AAPS J.* **2010**, *12*, 492.